ENGINEERING RESEARCH JOURNAL (ERJ)
Vol. 51, No. 4 October. 2022, pp.96-105
Journal Homepage: http://erj.bu.edu.eg

Lagrangian Simulation for Heat Transfer Enhancement Using Phase Change Slurry inside Channel with Constant Heat Flux

Hassan Salem [a *], Ehab Mina [b], Raouf Abdelmessih [c], Tarek Mekhail [d]

[a] Mechanical Power Engineering Department, Ain Shams University, Faculty of Engineering, Cairo, Egypt.

[b] Assistant Professor, Mechanical Power Engineering Department, Ain Shams University, Cairo, Egypt.

[c] Professor, Mechanical Power Engineering Department, Ain Shams University, Cairo, Egypt.

[d] Professor, Energy Engineering Department, Aswan University, Aswan, Egypt.

* Corresponding author

Abstract

By contrast with conventional heat transfer fluids, the usage of Microencapsulated phase change material (MPCM) suspended in conventional cooling fluids such as water; has shown enhanced heat transfer characteristics. This is due to their higher apparent specific heat values when subjected to heating within their phase change temperature range. The present study investigates numerically the impact of using MPCM slurry on heat transfer coefficient, and pressure drop for laminar thermally developing flow inside rectangular channel subjected to constant heat flux. The MPCM slurry consists of MPCM particles suspended in water as a base coolant. Lagrangian model was used to simulate the transport of MPCM particles through the flow domain by using ANSYS-FLUENT solver. Furthermore, the thermophysical properties of the MPCM particle were defined through the implementation of User-Defined Functions (UDF) available in FLUENT solver. The simulation results were compared to experimental data found in the literature and showed good agreement. The effect of varying MPCM mass concentration inside the slurry was also investigated to record their effect on heat transfer, pressure drop, and channel temperature. It was found that the heat transfer coefficient of MPCM slurry was noticeably increased when compared to the single phase fluid (water), but this comes on the expense of severe increase in the pressure drop. Moreover, a significant drop in the upper channel wall temperature was achieved due to phase change process of the slurry.

Keywords : Lagrangian; Phase Change material; microcapsules; Multiphase, CFD.

Nomenclature		Subscripts	
C	specific heat [J kg^{-1} K^{-1}]	f	base fluid (water)
D,d	diameter [m]	p	particle
D_h	Channel hydraulic diameter [m]	c	core

F	Force [N]
g	Gravity [m.s^{-2}]
K	thermal conductivity [W m^{-1} K^{-1}]
K_b	Boltzmann's constant [1.38066. 10^{-23} J K^{-1}]
K_n	Knudsen number [-]
M	Mass [kg]
ṁ	Mass flow rate [kg s^{-1}]
Nu	Nusselt Number [-]
Pr	Prandtl number [-]
Q̇	Heat rate [kW]
q''_w	Wall heat flux [W.m^{-2}]
Re	Reynolds number [-]
T	Temperature [ºC]
t	Time [s]
U,u	Velocity [m s^{-1}]
X	Axial location [m]
x^*	Dimensionless axial distance [-]
Pr	Prandtl number [-]
h_m	Latent heat of particle core [kJ/kg]
s	shell
w	wall
b	bulk

Greek Letters

μ	dynamic viscosity [N S m^{-2}]
ϕ	Particles volume fraction [%]
ν	kinematic viscosity [m^2 S^{-2}]
ρ	density [kg m^{-3}]
ΔT_m	Melting temperature range [ºC]
λ	Mean free path of water molecules [nm]
β	MPCM mass fraction [%]

Abbreviations

MPCM	Microencapsulated phase change material
UDF	User Defined Functions
DPM	Discrete Phase Model
Avg	Average

1. Introduction

Due to recent developments in microencapsulation manufacturing technology, the concept of preparing slurry in which microcapsules having phase change properties are dispersed in a carrier fluid has been presented [1]. When the suspended microcapsule change its phase from solid to liquid, a tremendous amount of heat can be absorbed with minimum temperature increase. For the same heat input to the system, utilizing Microencapsulated Phase Change (MPCM) particles suspension can be potentially used in heat transfer systems which require limited temperature change and also can provide advantage in applications with space restrictions [2, 3]. MPCM slurries are formed by the dispersion of microcapsules inside a base fluid such as water. The microcapsule is made up of an exterior shell and a phase change substance contained within the particle core as shown in Fig. 1. MPCM slurries have been widely implemented in thermal systems that require heat transfer fluids with enhanced thermal characteristics. This is attributed to higher apparent specific heat capacity of such slurries when compared to conventional heat transfer fluids with only sensible heating capabilities without phase change.

During the past 30 years, several attempts have been made to evaluate the potentials of using MPCM particles suspension in thermal systems. In the study of Chen et al. [2], they investigated the benefits of implementation of MPCM slurries in solar and waste heat systems applications. They reported an enhancement in heat transfer coefficient with about 2-3 times when compared to single phase flow of water. Another study performed by Charaunyakorn et al. [4], they developed a numerical model to investigate the laminar flow characteristics of MPCM slurry inside a circular duct with constant heat flux. The results showed an increase in Nusselt number with about 2-4 times when compared to flow of single phase fluid.

Goel et al. [5] experimentally reported a reduction of more than 50% in the circular duct temperature when compared to the single phase flow for the same flow conditions. There are number of studies found in literature that numerically investigated the laminar flow of MPCM slurry inside circular ducts [6-9, 30], while the turbulent flow of such slurries have been also discussed in several studies [10-12]. In the experimental study of Choi et al. [10], they reported

significant increase in heat transfer coefficient as a result of melting of phase change material for 10% particle mass concentration inside the mixture as well as increasing in the pressure drop with about 30% relative to single phase flow. In the experimental study of Wang et al. [11], they investigated the heat transfer behavior of forced flow of MPCM slurry in both laminar and turbulent flow conditions. They demonstrated the effect of heating rates and mass concentrations of microcapsule on the heat transfer performance and pressure drop. Using only 2% mass concentration of microcapsules, they reported an increase in the Nusselt number of about 40% relative to water flow.

Another experimental study performed by Yamagishi et al. [12], they recorded the change in both local heat transfer coefficient and pressure drop for turbulent slurry flow inside a horizontal circular pipe with constant heat flux. They concluded that the percentage increase in heat transfer coefficient depends greatly on the degree of turbulence, heating rate on tube wall, and the particles mass concentration. Inaba et al. [13] reported experimentally an increase in the average heat transfer coefficient for MPCM slurry with about 2-3 times compared to base water flow in both laminar and turbulent flow conditions. By incorporating MPCM particles inside a base coolant such as water flowing in cooling channels, the resulting fluid structure can be useful in providing optimum cooling performance for many applications with intensified thermal loads such as concentrated solar and photovoltaic systems as discussed by many researchers [14-16, 28, 29]. The current study specifically aims to highlight the basics of modeling strategies of such flows as used in cooling applications.

2. PROBLEM DESCRIPTION

Figure 1 shows a description for the physical domain for the problem under investigation which is represented by three-dimensional flow inside the rectangular channel with a constant heat flux applied at top of channel. The thermally developing flow inside the passage consists of a mixture of water as the base coolant and dispersed microcapsules each of which consists of outer shell and a phase change material inside the core of the particle as shown in Fig. 1.

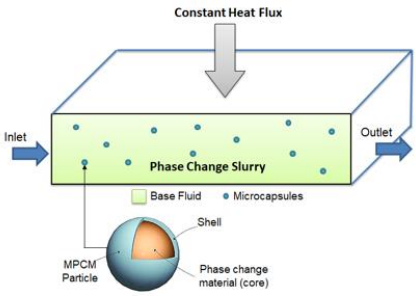

Fig. 1 Problem physical description.

For the available commercial computational packages, there are no direct multiphase models to simulate the phase change process of microcapsules. Theoretically, multiphase modeling of such flow can be performed by using either Eulerian-Eulerian (Mixture) approach or Eulerian-Lagrangian approach. The particles trajectories through the flow passage can be modeled by using Discrete Phase Model (DPM). Using DPM approach, the particle's motion can be predicted by applying Newton's second law of motion on each particle which is driven through the flow domain by the action of flow forces. The interaction (coupling) between the dispersed phase (microcapsule) and the continuous phase (water) can be performed by linking both phases through an interphase exchange of momentum and energy source terms that appear in the continuous phase governing equations.

The effect of the phase change process of microcapsule could be incorporated by altering the specific heat of the particle within the melting temperature range of the core material. This could be done numerically by using commercial CFD package such as FLUENT by the implementation of several User-defined Functions (UDF) programmed in C-language such that the particle specific heat can be changed when it is subjected to heating within the melting temperature range of the core material. Figure 2 shows the computational domain with the overall dimensions and the assigned boundary conditions.

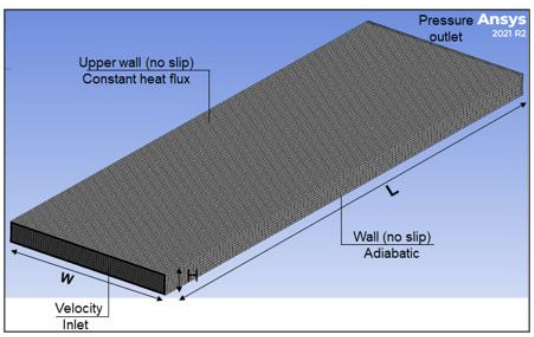

Fig. 2 Computational domain with boundary conditions, [L, W, H] = [1.5, 0.5, 0.1] (m)

3. PROPERTIES OF MPCM SLURRY

The thermophysical properties of both the microcapsule and base fluid are summarized in Table 1. In the current study, the microcapsule is composed of a core material which is Paraffin wax (n-eicosane) with a shell material of polymethylmethacrylate (PMMA) with average thickness of 0.3 µm and an average particle size of 10 µm. The particle core starts melting at a temperature of 34 ºC with a latent heat of melting of 247 kJ/Kg [17]. The thermophysical properties such as density, specific heat, and thermal conductivity of the microcapsule will be derived based on the composition of the particle constitutes. The density and the specific heat are derived using mass and energy conservation respectively as:

$$\rho_p = \frac{(1+Y)\rho_c\rho_s}{\rho_s + Y\rho_c} \quad (1)$$

$$C_p = \frac{(C_c + YC_s)\rho_c\rho_s}{(Y\rho_c + \rho_s)\rho_p} \quad (2)$$

where Y is the weight ratio of the core to shell.

Regarding the core material, the value of core density is taken as the average of its solid and liquid densities as there is no much difference between them. The specific heat of particle core will be evaluated according to its phase which will be either in liquid state, solid state, or changing phase within its melting temperature range. In the study of Alisetti and Roy [18], the authors suggested various profiles for calculating the effective specific heat of the particle core during the phase change stage such as Sine and rectangular profiles. They also reported that the difference between solutions was less than 4%. Consequently; for simplicity; the rectangular profile was selected in this study as shown in Fig. 3.

Table 1 Thermophysical properties of mixture components [17]

Material	Density ($Kg.m^3$)	Specific heat ($J.kg^{-1}C^{-1}$)	Thermal conductivity ($W.m.C^{-1}$)	Latent heat ($kJ.kg^{-1}$) h_m	Viscosity (Pa. s) at 20 °C
Paraffin wax (Core solid)	820	1920	0.212	247	-
Paraffin wax (Core liquid)	780	2460	0.16	-	-
PMMA (shell)	1180	1440	0.184	-	-
Water	998	4183	0.599	-	0.00112

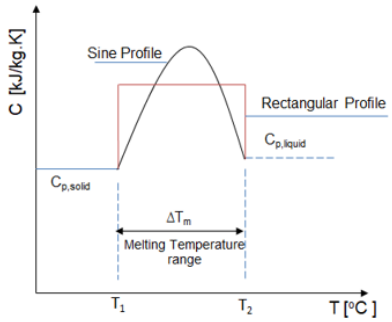

Fig. 3 Specific heat of particle's core as function of temperature.

Therefore, the calculation of the particle's core specific heat will be calculated based on the following profile (see Fig. 3):

If $T < T_1$

$$C_{p,c} = C_{p,c}\,(solid) \quad (3)$$

Else if $T_1 \leq T < T_2$

$$C_{p,c} = C_{p,c(avg)} + \left(\frac{h_m}{\Delta T_m}\right) \quad (4)$$

Else $T \geq T_2$

$$C_{p,c} = C_{p,c}\,(liquid) \quad (5)$$

The switching between different specific heat formulas is performed by using the UDF which was programed and linked to the FLUENT solver such that to get the cell temperature from the solver and selection is performed for the appropriate specific heat formula based on the returned temperature value. The thermal conductivity of the microcapsule was calculated based on composite sphere method as given by [19]:

$$\frac{1}{k_p d_p} = \frac{1}{k_c d_c} + \frac{d_p - d_c}{k_s d_p d_c} \quad (6)$$

Table 1 gives the value of thermal conductivity for both core and shell material, while the ratio of particle core diameter to outer particle diameter is calculated as follows:

$$\left(\frac{d_c}{d_p}\right)^3 = \frac{\rho_s}{\rho_s + Y\rho_c} \quad (7)$$

4. GOVERNING EQUATIONS

The flow through the channel was modeled using the full Navier-Stokes equation for three-dimensional, viscous, incompressible laminar flow along with continuity and energy equations as follows:

$$\nabla.\left(\rho_f\vec{V}\right) = 0 \quad (8)$$

$$\nabla.\left(\rho_f\vec{V}\vec{V}\right) = -\nabla P + \nabla.\left(\mu_f\nabla\vec{V}\right) + S_m \quad (9)$$

$$\nabla.\left(\rho_f\vec{V}C_fT\right) = \nabla.\left(k_f\nabla T\right) + S_e \quad (10)$$

where S_m and S_e are the interphase exchange source terms for momentum and energy, respectively which are defined as follows [20]:

$$S_m = \frac{1}{\delta V}\sum_{p=1}^{p=n} F_p \quad (11)$$

$$S_e = \frac{1}{\delta V}\sum_{p=1}^{p=n} m_P C_p \frac{dT}{dt} \quad (12)$$

where (n)is the total number of particles that exist in a fluid cell of volume δV.

The particle trajectory is predicted by integrating the force balance equation per unit particle mass which is written in a Lagrangian reference frame as [21]:

$$\frac{du_p}{dt} = \frac{18\mu_f(u_f - u_p)}{\rho_p D_p^2 C_c} + \frac{(\rho_p - \rho_f)g}{\rho_p} + F_x \quad (13)$$

where C_c is Cunningham correction factor which is defined as [21]:

$$C_c = 1 + \frac{2\lambda}{d_p}\left(1.257 + 0.4e^{-\left(\frac{1.1d_p}{2\lambda}\right)}\right) \quad (14)$$

As shown in Equation (13), particle inertia on the left hand side is equated to the sum of forces acting on the particle on the right hand side per unit particle mass. The first and second terms on the right hand side is the drag force and gravity per unit particle mass, respectively. While, the third term is an additional acceleration term which indicates all other additional forces which may be included according to the attendant flow physics. The particles in the flow field are assumed to be spherical particles throughout this study. The identification of the forces that may affect the particle motion is extremely important for accurate prediction of the particle trajectory. The particle motion is also influenced by the Thermophoresis force; which is the force caused by temperature gradient in the flow field as given by Talbot et al. [22]:

$$F_{Th} = \frac{6\pi d_p\mu^2 C_1\left(\frac{k_f}{k_p} + C_tK_n\right)}{\rho(1 + 3C_2K_n)\left(1 + 2\left(\frac{k}{k_p}\right) + 2C_tK_n\right)}\frac{1}{m_pT}\nabla T \quad (15)$$

where; K_n is the Knudsen number = $2\lambda/d_p$, C_1 is thermal slip coefficient = 1.17, C_2 is momentum exchange coefficient = 1.14, and C_t is temperature jump coefficient = 2.18.

When a particle moves in a shear layer, it may be subjected to a lift force which is known as Saffman's lift force which is given as [21]:

$$F_L = \frac{2K\,\nu^{\frac{1}{2}}\rho\, d_{ij}}{\rho_p d_p (d_{lk}d_{kl})^{\frac{1}{4}}}(\vec{u} - \vec{u}_p) \quad (16)$$

where $K = 2.59$ is the constant coefficient of Saffman's lift force and d_{ij} is the rate deformation tensor defined as [21]:

$$d_{ij} = \frac{1}{2}\left(u_{i,j} + u_{j,i}\right) \quad (17)$$

The particle motion is also influenced by pressure gradient force given by [21]:

$$F_P = \left(\frac{\rho_f}{\rho_p}\right)\overrightarrow{u_p}.\nabla\overrightarrow{u_f} \quad (18)$$

Also, the particles are exchanging heat with the Eulerian phase (water). The particles can be considered as a lumped system due to their small size. Therefore, the energy balance equation for a particle can be written as:

$$m_pC_p\frac{dT}{dt} = h\,A_p\left(T_f - T_p\right) \quad (19)$$

The particle specific heat is calculated based on Equation (2), and the heat transfer coefficient h is calculated from Ranz and Marshall's correlation [21]:

$$Nu = \frac{h\,d}{k_f} = 2 + 0.6\,Re_p^{\frac{1}{2}}\,Pr^{\frac{1}{3}} \quad (20)$$

Where the particle Reynolds number Re_p is defined as:

$$Re_p = \frac{\rho_f|u_f - u_p|D_p}{\mu_f} \quad (21)$$

Moreover, the bulk Reynolds number is defined as:

$$Re_b = \frac{\rho_b V D_h}{\mu_b} \quad (22)$$

where the bulk density ρ_b, viscosity μ_b, and thermal conductivity k_b are estimated according to [23, 24]:

$$\rho_b = \frac{\rho_p\rho_f}{\beta\rho_f + (1-\beta)\rho_p} \quad (23)$$

$$\frac{\mu_b}{\mu_f} = (1 - \phi - 4.45\,\phi^2)^{-2.5} \quad (24)$$

$$\frac{k_b}{k_f} = \frac{2k_f + k_p + 2\phi(k_p - k_f)}{2k_f + k_p - \phi(k_p - k_f)} \quad (25)$$

where β is the mass fraction of particles inside the slurry, and ϕ is the volumetric fraction of particles inside the slurry which is related to mass fraction by [23]:

$$\phi = \beta\left(\frac{\rho_b}{\rho_p}\right) \quad (26)$$

The bulk local convection coefficient h_x is defined as:

$$h_x = \frac{q''_w}{(T_{w,x} - T_{b,x})} = \frac{\frac{Q_w}{\pi D_h L}}{(T_{w,x} - T_{b,x})} = \frac{Nu_x k_b}{D_h} \quad (27)$$

where $T_{w,x}$ is the average local span-wise wall temperature at a particular axial location, and $T_{b,x}$ is defined as the mass weighted average of fluid temperature over the cross section at that location. The dimensionless axial distance x^* is defined as:

$$x^* = (x/D_h)/(Re \cdot Pr) \quad (28)$$

where x is the axial distance, and D_h is the hydraulic diameter of the flow channel.

5. RESULTS AND DISCUSSION

5.1 GRID SENSITIVITY ANALYSIS

Firstly, a grid sensitivity analysis was performed grid sensitivity analysis using the concept of Grid Convergence Index (GCI) as explained by McHale et al. [27]. Three different structured mesh resolutions were tested with a number of divisions of 70x30x650, 75x40x700, and 85x45x700. A safety factor of 1.2 was used with estimated order of accuracy of 2.12. The change in GCI ratio for two successive meshes was about 1.006; approaching the theoretical value of 1; which indicates that the simulation results are well converged. The change in Nusselt number for the tested meshes was selected as a comparison criteria as shown in Fig. 4. All the simulations were performed using water at the same Reynolds number of 250, inlet fluid temperature of 25 ºC, and constant heat flux of 1000 W/m2 applied at top of the flow passage. As it can be noticed from Fig. 4, the second and third meshes provided similar results, showing that the numerical simulations converged to the same values.

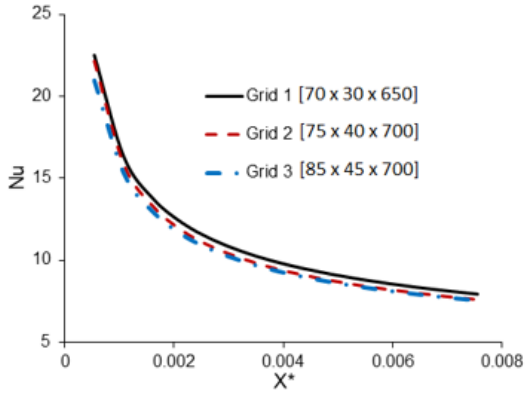

Fig. 4. Grid independence study for channel flow.

5.2 MODEL VALIDATION

To assess the validity of the numerical simulation for the MPCM slurry, a comparison was performed made against the experimental work of Chen et al. [23] and Wang et al. [24]. In the study of Wang et al. [24], they investigated experimentally the increase in heat transfer coefficient for MPCM slurry for thermally developing laminar flow in circular duct with constant heat flux. Wang et al. [24] and Chen et al. [23] used the same test rig dimensions and also the same particle properties. Moreover, they used particle core material which is industrial-grade 1-bromo-hexadecane (C16H33Br) with a melting temperature of 14.3 ºC and a latent heat of melting of 160 kJ/Kg as measured by Differential Scanning Calorimeter (DSC) [24] with average particle size of 10 µm.

Figure 5 shows the local axial variation of Nusselt number for water and MPCM slurry with a mass fraction of 15.8% , total wall heat rate of 296 Watt, and Re=1200. It can be noticed that the results of numerical work have good agreement with the experimental data. It can be also noticed that there is an increase in the local Nusselt number with more than 40% with respect to pure water. In the study of Chen et al. [23], they measured the axial variation for both bulk and wall temperature for MPCM slurry with a mass fraction of 15.8%, Re = 416, and constant wall heat flux of 14,440 W/m2. Figure 6 shows a comparison between experimental and numerical results for the axial variation of bulk and wall temperatures as predicted by DPM.

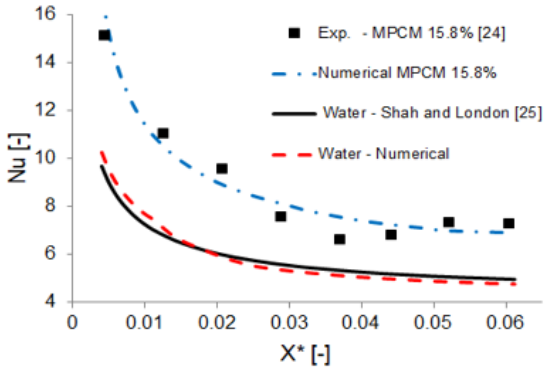

Fig. 5 Local variation of Nusselt number for water and MPCM slurry for β =15.8%, Re =1200, and Q =296 W.

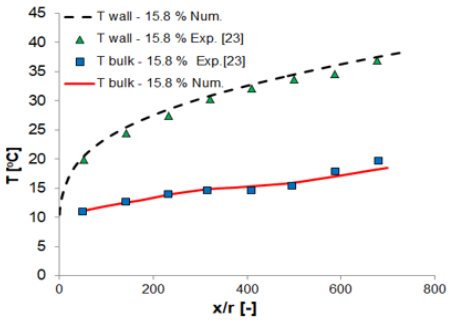

Fig. 6 Local variation for wall and bulk temperature for MPCM slurry for β.=15.8%, Re =416, and q_w^"=14,440 W/m2

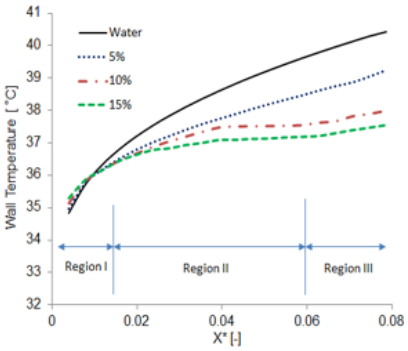

(b)

Fig. 7 Results for Re =500, q''_w=1000 W/m^2 at various MPCM mass concentrations (a) Local convection coefficient, (b) Upper wall temperature.

5.3 EFFECT OF MPCM SLURRY ON HEAT TRANSFER AND PRESSURE DROP

After validating the numerical model, several numerical simulations were performed to assess the effect of various parameters on heat and flow characteristics. The most effective parameter which may influence the performance is the particles mass concentration. Figures 7(a) and 6(b) show the effect of varying the particles mass concentration on convection coefficient and upper wall temperature, respectively. The flow domain can be thought as divided into 3-regions as indicated in Fig. 7(a); pre-phase change region (region I), phase change region (region II), and post-phase region (region III). For region I, Fig. 7(a) indicates that introducing microcapsules inside the base fluid has caused some reduction in heat transfer coefficient, and this reduction increases as particles concentration increases. This may be attributed to lower thermal properties of the mixture in this region, such as specific heat and thermal conductivity due to the presence of the microcapsules in its solid state. Once the microcapsules enter region II within a temperature field that permits the onset of phase change process, a large amount of heat is drawn from the base fluid as a result of the phase change process which subsequently causes a reduction in wall temperature as it can be shown in Fig. 7(b).

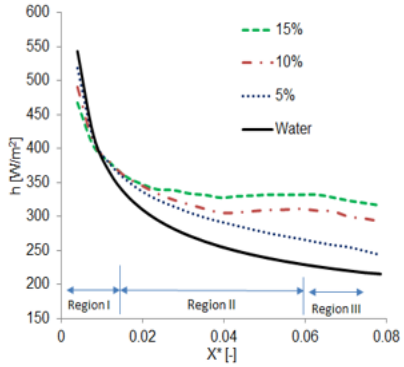

(a)

The bulk temperatures as shown in Fig. 8(a) are obtained by averaging the bulk temperature over the cross section at various axial locations, that's why the temperature variation inside region II deviates a little from the flattened behavior as a result of the averaging process as the fluid layer affected by the phase change process only exists near the upper surface. Figure 8(b) also shows the particles trajectories colored by specific heat values in region II which indicates a tremendous increase in the particles specific heat near the upper wall due to the phase change process.

It can be also shown from Fig. 9 that the pressure drop has been increased due to the presence of the microcapsules inside the base fluid. This is attributed to the increased interaction between the particles with both the base fluid and the bounding walls. As reported by [20], the bulk slurry viscosity greatly increases by the increase in particles mass concentration [20].

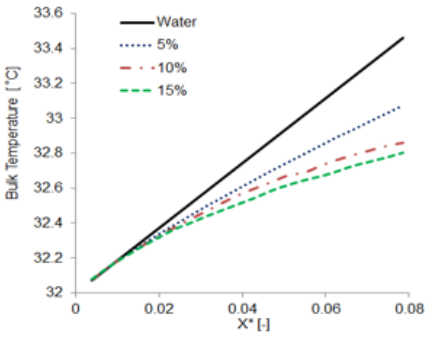

(a)

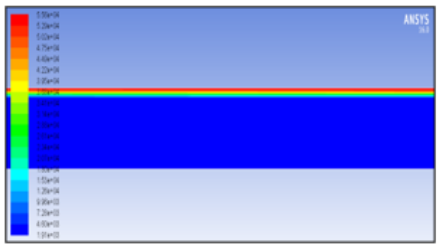

(b)

Fig. 8 (a) Change in MPCM slurry (bulk) temperature for Re =500, $\mathbf{q''_w}$=1000 W/m^2 at various MPCM mass concentrations, (b) Contours of particles specific heat inside region II at 5% mass concentration.

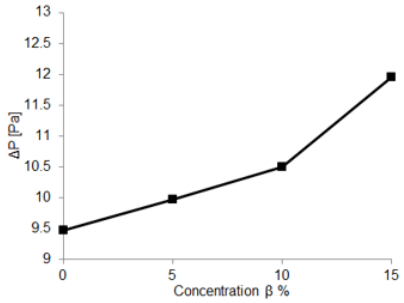

Fig. 9 Change in pressure drop for MPCM slurry for Re =500, q_w^\"=1000 W/m2 at various MPCM mass concentrations for the same volumetric flow rate.

Figure 10 shows the net enhancement in average heat transfer coefficient of the slurry $\bar{h}_{MPCM}$ as a function of particle concentration relative to base fluid $\bar{h}_{water}$.The heat transfer coefficient has been increased up to 25 % for a particles concentration of 15 %. As demonstrated by [26], it was shown that the Newtonian assumption can be assumed up to 20% particles concentration, therefore there is an upper limit for the validity of the Newtonian assumption in modeling procedure.

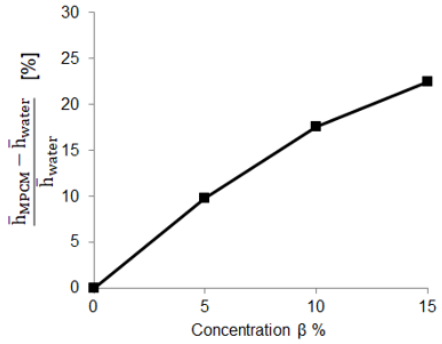

Fig. 10 Relative increase in average convection coefficient for Re =500, $\mathbf{q''_w}$=1000 W/m^2 at various MPCM mass concentrations.

To demonstrate the effect of the relative importance of both heat transfer rate and pumping power, numerical investigations were performed with a target of limiting the outlet fluid temperature at 35 ºC using both water and phase change slurry. The fluid inlet temperature was fixed at 32 ºC. Therefore, the temperature difference across the channel was fixed, and the flow rate was altered to record how much flow is needed for the same heat load using water only and MPCM slurry. The heat transfer rate and pumping power were calculated for various mass flow rates using the following equations:

$$\dot{Q} = \dot{m}\, C_b\, \Delta T \quad (29)$$

$$\dot{W}_p = \frac{\dot{m}}{\rho_b}\, \Delta P \quad (30)$$

where $\dot{Q}$ is the heat transfer rate [W] and $\dot{W}_p$ is the pumping power [W].

The bulk specific heat for the slurry C_b can be evaluated based on energy balance as [23]:

$$C_b = \beta C_p + (1-\beta) C_f \quad (31)$$

It can be noticed from Fig. 11 that the pumping power requirements for the MPCM slurry decrease significantly for the larger heat transfer rate when compared to base fluid as a result of higher apparent specific heat capacity due to phase change process of microcapsules. For particle concentration of 15% and heat transfer rate of 6 kW, the pumping consumption could be reduced to about 62% as compared to base water. This has the advantages of reducing the system size for the same heat input. Moreover; for the same heat input to the system; larger mass flow rate will be required if only water is only used a heat transfer fluid, which subsequently leads to a larger pumping power requirements when compared to MPCM slurry.

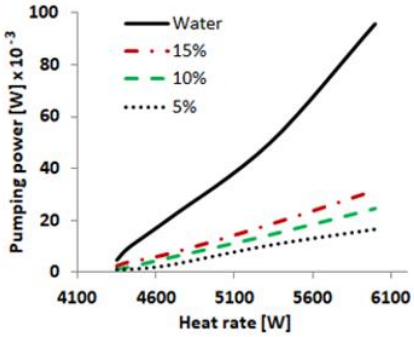

Fig. 11 The pumping consumption versus heat transfer rates at various concentrations.

6. CONCLUSION

The present study has numerically investigated the flow and heat transfer characteristics for three-dimensional laminar flow of MPCM slurry inside the rectangular channel with constant heat flux with the aim of discussing the effect of various parameters on heat transfer coefficient and pressure drop. The following conclusions could be derived from the study's findings:

- When compared to experimental data, the numerical model adequately predicted heat transfer coefficient for the MPCM slurry flow
- Nusselt number has been greatly enhanced when compared to single phase flow of water inside the cooling channel at the same Reynolds number
- Higher pressure drop was observed for MPCM slurry when compared to single flow of water at the same Reynolds number
- The upper heated wall temperature has been significantly reduced as a result of higher heat capacity of MPCM slurry
- Large heat transfer rates could be achieved using MPCM slurry with lower mass flow rate and pumping power requirements compared to water flow

Future research should consider the effect of turbulent flow on Nusselt number and pressure drop.

7. References

[1] Mehalick, E. M., and A. T. Tweedie. "*Two component thermal storage material study phase II. Final report*. " No. COO-2845-78/2. General Electric Co., Philadelphia, PA (USA). Space Div., 1979.

[2] Kasza, K. E., and M. M. Chen. "Improvement of the performance of solar energy or waste heat utilization systems by using phase-change slurry as an enhanced heat-transfer storage fluid." *Journal of Solar Energy Engineering* 107 (1985) 229–236.

[3] Chen, Binjiao, Xin Wang, Yinping Zhang, Hui Xu, and Rui Yang. "Experimental research on laminar flow performance of phase change emulsion." *Applied thermal engineering* 26, no. 11-12 (2006): 1238-1245.

[4] Charunyakorn, Pongtorn, S. Sengupta, and S. K. Roy. "Forced convection heat transfer in microencapsulated phase change material slurries: flow in circular ducts." *International journal of heat and mass transfer* 34, no. 3 (1991): 819-833.

[5] Goel, Manish, Sanjay K. Roy, and Subrata Sengupta. "Laminar forced convection heat transfer in microcapsulated phase change material suspensions." *International journal of heat and mass transfer* 37, no. 4 (1994): 593-604.

[6] Zhang, Yuwen, and Amir Faghri. "Analysis of forced convection heat transfer in microencapsulated phase change material suspensions." *Journal of thermophysics and heat transfer* 9, no. 4 (1995): 727-732.

[7] Alisetti, Edwin L., and Sanjay K. Roy. "Forced convection heat transfer to phase change material slurries in circular ducts." *Journal of thermophysics and heat transfer* 14, no. 1 (2000): 115-118.

[8] Hu, Xianxu, and Yinping Zhang. "Novel insight and numerical analysis of convective heat transfer enhancement with microencapsulated phase change material slurries: laminar flow in a circular tube with constant heat flux." *International Journal of Heat and Mass Transfer* 45, no. 15 (2002): 3163-3172.

[9] Ho, Ching-Jenq, J. F. Lin, and S. Y. Chiu. "Heat transfer of solid–liquid phase-change material suspensions in circular pipes: effects of wall conduction." *Numerical Heat Transfer, Part A* 45, no. 2 (2004): 171-190.

[10] Eunsoo, Choi, Young I. Cho, and Harold G. Lorsch. "Forced convection heat transfer with phase-change-material slurries: turbulent flow in a circular tube." *International journal of heat and mass transfer* 37, no. 2 (1994): 207-215.

[11] Wang Y, Chen Z, Ling X. "An experimental study of the latent functionally thermal fluid with micro-encapsulated phase change material particles flowing in microchannels. " *Applied Thermal Engineering* 2016;105:209–16..

[12] Yamagishi, Yasushi, Hiromi Takeuchi, Alexander T. Pyatenko, and Naoyuki Kayukawa. "Characteristics of microencapsulated PCM slurry as a heat-transfer fluid." *AichE journal* 45, no. 4 (1999): 696-707.

[13] Inaba, Hideo, Myoung-Jun Kim, and Akihiko Horibe. "Melting heat transfer characteristics of microencapsulated phase change material slurries with plural microcapsules having different diameters." *J. Heat Transfer* 126, no. 4 (2004): 558-565.

[14] Liu, Lingkun, Yuting Jia, Yaxue Lin, Guruprasad Alva, and Guiyin Fang. "Performance evaluation of a novel solar photovoltaic–thermal collector with dual channel using microencapsulated phase

change slurry as cooling fluid." *Energy Conversion and Management* 145 (2017): 30-40.

[15] Jia, Yuting, Chuqiao Zhu, and Guiyin Fang. "Performance optimization of a photovoltaic/thermal collector using microencapsulated phase change slurry." *International Journal of Energy Research* 44, no. 3 (2020): 1812-1827.

[16] Qiu, Zhongzhu, Xiaoli Ma, Xudong Zhao, Peng Li, and Samira Ali. "Experimental investigation of the energy performance of a novel Micro-encapsulated Phase Change Material (MPCM) slurry based PV/T system." *Applied energy* 165 (2016): 260-271.

[17] Dammel, Frank, and Peter Stephan. "Heat transfer to suspensions of microencapsulated phase change material flowing through minichannels." *Journal of heat transfer* 134, no. 2 (2012).

[18] Alisetti, Edwin L., and Sanjay K. Roy. "Forced convection heat transfer to phase change material slurries in circular ducts." *Journal of thermophysics and heat transfer* 14, no. 1 (2000): 115-118.

[19] Guyer, Eric C. *Handbook of applied thermal design*. CRC press, 1999.

[20] Mirzaei, Mostafa, Majid Saffar-Avval, and Hamid Naderan. "Heat transfer investigation of laminar developing flow of nanofluids in a microchannel based on Eulerian–Lagrangian approach." *The Canadian journal of chemical engineering* 92, no. 6 (2014): 1139-1149.

[21] Albojamal, Ahmed, and Kambiz Vafai. "Analysis of single phase, discrete and mixture models, in predicting nanofluid transport." *International Journal of Heat and Mass Transfer* 114 (2017): 225-237.

[22] Talbot, L. R. K. R. W. D. R., R. K. Cheng, R. W. Schefer, and D. R. Willis. "Thermophoresis of particles in a heated boundary layer." *Journal of fluid mechanics* 101, no. 4 (1980): 737-758.

[23] Chen, Binjiao, Xin Wang, Ruolang Zeng, Yinping Zhang, Xichun Wang, Jianlei Niu, Yi Li, and Hongfa Di. "An experimental study of convective heat transfer with microencapsulated phase change material suspension: laminar flow in a circular tube under constant heat flux." *Experimental Thermal and Fluid Science* 32, no. 8 (2008): 1638-1646.

[24] Wang, Xichun, Jianlei Niu, Yi Li, Xin Wang, Binjiao Chen, Ruolang Zeng, Qingwen Song, and Yinping Zhang. "Flow and heat transfer behaviors of phase change material slurries in a horizontal circular tube." *International journal of heat and mass transfer* 50, no. 13-14 (2007): 2480-2491.

[25] Shah, R. K., and A. L. London. "Laminar Flow Forced Convection in Ducts, Academic Press, New York, 1978."

[26] Ayel, V., O. Lottin, and H. Peerhossaini. "Rheology, flow behaviour and heat transfer of ice slurries: a review of the state of the art." *International Journal of Refrigeration* 26, no. 1 (2003): 95-107.

[27] McHale, M., Friedman, J., Karian, J. "Standard for Verification and Validation in Computational Fluid Dynamics and Heat Transfer: An American National Standard" *American Society of Mechanical Engineers*, VV20 (2009-R2021), ISBN: 9780791832097.

[28] Kondle, S., Alvarado, J. L., Marsh, C. "Laminar flow forced convection heat transfer behavior of a phase change material fluid in microchannels." Journal of heat transfer 135.5 (2013).

[29] Alvarado, J. L., Marsh, C., Sohn, C., Phetteplace, G., Newell, T. "Thermal performance of microencapsulated phase change material slurry in turbulent flow under constant heat flux." International journal of heat and mass transfer 50.9-10 (2007): 1938-1952.

[30] Ravi, G., Alvarado, J. L., Marsh, C., Kessler, D. A."Laminar flow forced convection heat transfer behavior of a phase change material fluid in finned tubes." Numerical Heat Transfer, Part A: Applications 55.8 (2009): 721-738.